Hall Thruster Microscopic Processes : Qualifying 2D PIC Simulations against Collective Scattering Experimental Data

C. Honoré[1], A. Héron[2], S. Tsikata[1], D. Grésillon[1], N. Lemoine[3]

[1] *Laboratoire de Physique des Plasmas CNRS-UPMC, École Polytechnique, Palaiseau France*

[2] *Centre de Physique Théorique, École Polytechnique, Palaiseau, France*

[3] *Institut Jean Lamour, Université Henri Poincaré, Nancy, France*

Hall thruster performance improvement requires a good understanding of electron transport through the ion acceleration zone. In this zone, electrons are confined thanks to a permanent radial magnetic field. The electron mobility in the axial direction is higher than predicted by collisional models. Small scale instabilities could be a good candidate for explaining this anomalous transport.

Collective scattering measurements performed in front of a Hall thruster [3] showed the presence of small scale (mm) fluctuation modes in the azimuthal, ExB drift direction as foreseen by linear models [1, 2]. We compare these observations with 2D axial-azimuthal PIC simulations.

Collective Scattering (CS) measurements

The collective light scattering diagnostic is non perturbative. It measures electron density fluctuation at a specific wave vector. The scattered electric field is proportional to the spatial Fourier transform at the scattering wave vector, $\vec{k}$, of the electron density inside the scattering volume V : $n(\vec{k},t) = \int_V n(\vec{r},t)e^{-i\vec{k}.\vec{r}}d^3\vec{r}$. This scattering wave vector is determined through the Bragg relation by the laser's initial mono-mode wave vector $\vec{k}_i$ and the scattering angle θ. Fluctuation intensity is evaluated by the form factor, defined as scattering signal mean quadratic value : $S(\vec{k}) = \langle|n(\vec{k},t)|^2\rangle_t / n_0 V$ (n_0 is the volume mean density).

In order to access millimeter scale instabilities in this low density plasma, a high power CO_2 laser is used as the initial primary beam. Forward scattering is observed at small (10 mrad) angle θ. The measurement volume is placed at least 5 mm in front of the thruster channel exit

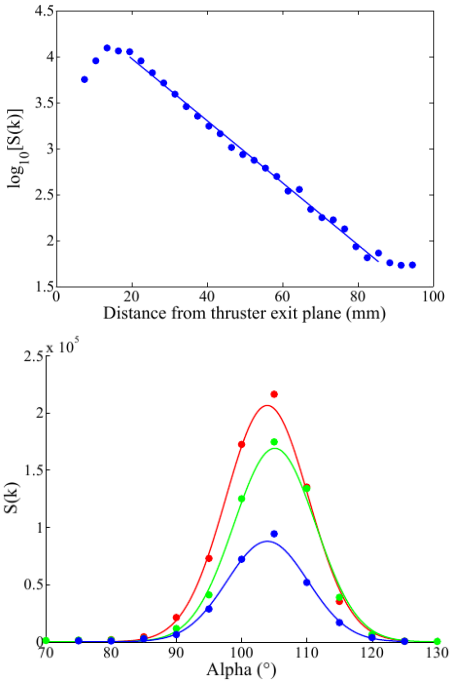

Fig. 1: CS form factor vs axial position (a) and orientation (b)

plane. Heterodyne detection is used to improve diagnostic sensitivity and to retain scattering signal phase information.

Collective scattering measurements have shown that an azimuthal millimetric mode is present. Figure 1a shows how this mode's intensity varies along the thruster axis. The mode amplitude increases until 13 mm in front of the thruster exit plane, then decreases exponentially.

This mode is not purely azimuthal. In figure 1b, α is the wave vector angle in the axial-azimuthal plane ($\alpha = 90^o$ for the azimuthal direction). Measured for different heights in the thruster, the form factor is largest at $\alpha \sim 105^o$. The mode has an axial component, oriented towards the thruster.

Axial and azimuthal 2D PIC simulation

In order to estimate small scale density fluctuations inside the thruster, an axial (x) and azimuthal (y) 2D PIC simulation was performed. The magnetic field is imposed. It is perpendicular to the x-y plane and varies along the axis with a maximum value of 170 G at $x = 25$ mm. The electric acceleration is supplied by a imposed 300 V potential drop between the left ($x = 0$) and right ($x = 40$ mm) borders. Primary electrons flow from the right border. Ions and secondary electrons are created by collisions between the primary electrons and the neutral gas, treated as a fluid.

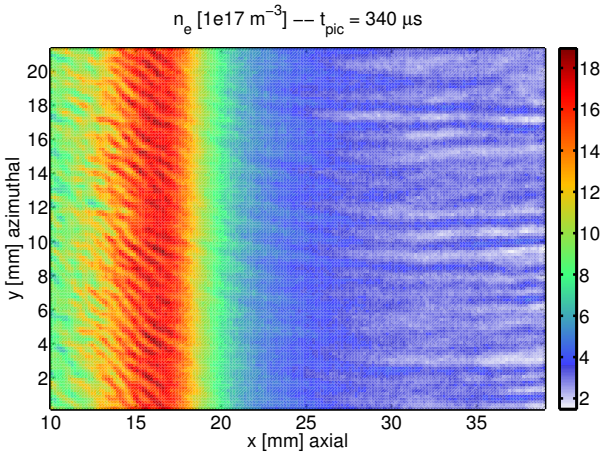

Fig. 2: PIC simulation electron density map at time 340μs

A typical electron density map for a simulation snapshot time is shown in figure 2. For $x \leq 17$ mm, the density increases mainly because of the ionization. For $x \geq 17$ mm, the density decreases because ions accelerate (while the ion flow rate is maintained). We observe millimetric structures mainly in the azimuthal direction. These structures seem of small size and are quite oblique in the ionization zone. The structures have a larger length scale in the acceleration zone. Their orientation changes from oblique to parallel to the azimuthal direction as ions accelerate. These structures have long correlation length along the axial direction in the acceleration zone. They appear to be convected by the ion flow.

We have applied to these simulated electron density fields the same local spatial Fourier transform as is performed for collective scattering data for each x and y position inside this plane and for a wide range of $\vec{k}$ vectors. Since simulation parameters are uniform along the

azimuthal direction, the simulated form factor is averaged along y.

Figure 3 shows the form factor variation with the wave vector k_x and k_y components, for two different axial positions. The first position ($x =$ 18 mm) (figure 3a) corresponds to the limit between the ionization and the acceleration zone. We observe that the form factor is large for a zone of k values above 6.3 rad mm^{-1} ($\lambda \leq 1$ mm) and for an oblique k direction around 60^o. These modes are observed for x positions inside the ionization zone. Another mode is observed with a smaller k value ($k \sim 5$ rad mm^{-1}, $\lambda \geq 1$ mm). This millimetric mode is observed along the acceleration zone with a varying $\vec{k}$ wave vector. The azimuthal component k_y is constant , but the axial component k_x decreases as x grows (and ions accelerate). A secondary mode appears with the same k_x value but larger k_y, around 5.2 rad mm^{-1}, moving the same direction. We observe both modes on figure 3b at the end of the acceleration zone ($x = 35$ mm). The k_x component becomes slightly negative.

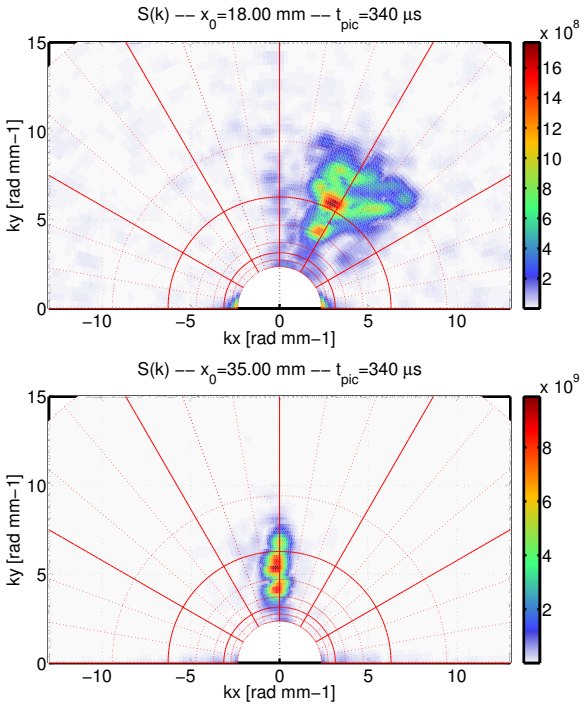

Fig. 3: PIC Form factor vs wave vector for $x = 18$ mm (a) & 35 mm (b)

This form factor is integrated over k in order to estimate the mode intensity variation with x. We show results for different simulation snapshot times (320 to 340μs) in order to show phenomenon stability. (figure 4). The intensity of the submillimetric mode decreases in the ionization zone. The millimetric mode grows along, and even beyond the end of the acceleration zone.

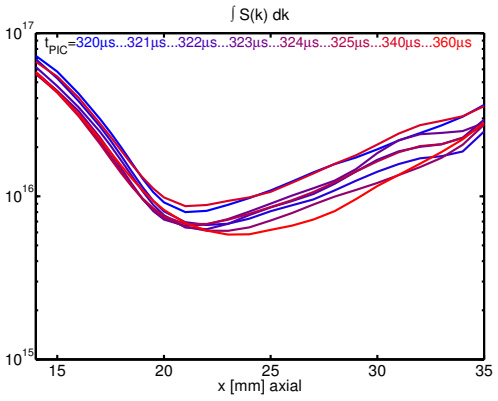

Fig. 4: PIC Density local variance vs axial position

Comparison between PIC simulation and collective scattering results

The closest approach of the scattering volume to the thruster exit plane is 5 mm. The position $x = 0$ for CS data corresponds to $x = 25$ mm for the PIC simulations (thruster exit plane). For both CS data (figure 1a) and the PIC simulation (figure 5a), purely azimuthal fluctuation mode amplitude

($k = 6.2$ rad mm^{-1}), continues to increase beyond the thruster exit plane.

As observed with CS data, the PIC millimetric mode is not purely azimuthal, but has a small axial component. In PIC simulation, the mode orientation varies along the thruster axis. The mode is oriented towards the thruster inside the acceleration zone. Beyond $x =$ 29 mm, the mode is directed outward. Since collective scattering measurements correspond to a position where mode orientation varies rapidly, orientation comparisons between the PIC results (figure 5b) and collective scattering observations (figure 1b) is difficult. Further collective scattering measurements are necessary to verify if the mode orientation follows the same trend as PIC simulations.

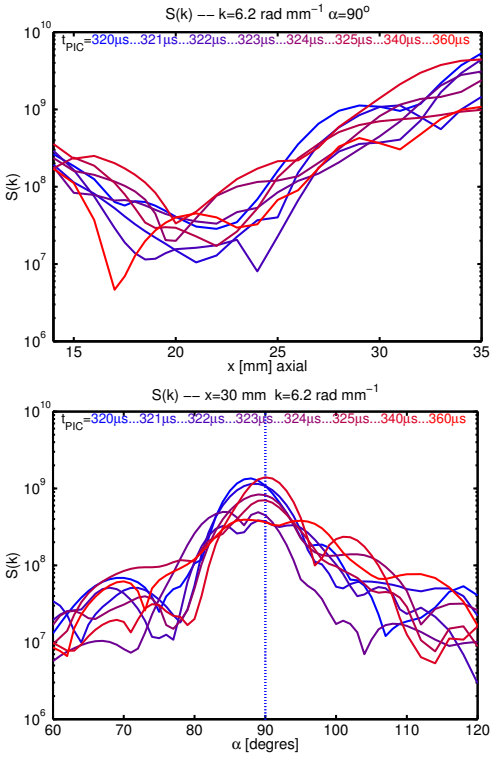

Fig. 5: PIC form factor vs axial position (a) and orientation (b)

Conclusion

As observed with collective scattering, an azimuthal millimetric mode is present in the axial-azimuthal 2D PIC simulation. Collective scattering experiments confirm that the mode amplitude continues to grow at the end of the acceleration zone.

Directivity analysis shows that the small scale mode seen by collective scattering is not purely azimuthal, but has a small axial inward component. 2D PIC simulations (with axial and azimuthal directions), also show an axial component in the same direction.

Acknowledgement : This work was performed in the framework of the collaborative-research program GdR 3161 CNRS-CNES-Snecma-Universities “Propulsion par Plasma dans l’Espace“

References

[1] J.-C. Adam et al., Phys. Plasmas **11**(2004), p285.

[2] A. Ducrocq et al., Phys. Plasmas **13**(2006), 102111.

[3] S. Tsikata et al., Phys. Plasmas **16**(2009), 035506.

[4] S. Tsikata, Ph D Thesis, Ecole Polytechnique (2009).